Influence of spin glass-like magnetic relaxation on the zero-field-cooled exchange bias effect

L. T. Coutrim,[1] E. M. Bittar,[2] F. Garcia,[2] and L. Bufaiçal[1,*]

[1]*Instituto de Física, Universidade Federal de Goiás, 74001-970, Goiânia, GO, Brazil*
[2]*Centro Brasileiro de Pesquisas Físicas, 22290-180, Rio de Janeiro, RJ, Brazil*

The zero-field-cooled exchange bias (ZEB) effect is a remarkable phenomenon recently reported for some reentrant spin glass-like compounds. In this work, the time evolution of magnetization is thoroughly investigated for two ZEB materials in order to figure out the role played by the spin glass-like phase on such effect. $La_{1.5}Sr_{0.5}CoMnO_6$ and $La_{1.5}Ca_{0.5}CoMnO_6$ were chosen as representative samples of ZEB systems, since the former compound presents the largest ZEB reported so far, while the second has a much smaller effect, despite being structurally/chemically similar. Comprehensive magnetic measurements were carried on both samples, and the results are discussed in terms of the amount and time evolution of the spin glass-like phase under the influence of a varying field. We also propose a phenomenological model, based on the pinning of spin glass-like moments and on the dynamics of their magnetic relaxation, to explain the asymmetry observed in the hysteresis loops. The good agreement between the simulated and experimental results confirms our hypothesis that the spin glass-like phase is key to the ZEB effect.

I. INTRODUCTION

Spin glass (SG) materials are significantly different from most condensed matter systems, such as conventional ferromagnets, liquid crystals, and superconductors. The fundamental difference is that for the latter systems, there are well-known symmetries that allow mathematical simplifications and physical insights, admitting easier physical modeling [1]. Conversely, SG presents quenched magnetic disorder, for which there is no evident long-range order, leading to nonobvious phase transitions and broken symmetries [2]. Therefore, the intriguing properties of SG, especially its dynamics, are not well understood yet [1–3].

Another subject of great academic and technological interest is the exchange bias (EB) effect, characterized by a shift of the magnetic hysteresis loop [$M(H)$] along the magnetic field (H) axis. Usually, this effect is ascribed to the unidirectional exchange anisotropy formed at the interfaces of antiferromagnetic (AFM) and ferromagnetic (FM)/ferrimagnetic (FIM) phases in heterogeneous systems, being conventionally observed after the system is cooled through its Néel temperature under an applied magnetic field [4]. This conventional EB (CEB) effect is a well-known phenomenon discovered around 60 years ago, and improvements in techniques for the production of heterostructures have renewed interest in it, enabling the manufacture of multifunctional devices using strongly correlated electronic materials [5].

SG and EB merge in recently discovered materials that display a shift of their hysteresis loop even when they are cooled from an unmagnetized state down to low temperature (T) in zero field. This is commonly referred to as the zero-field-cooled exchange bias (ZEB) effect. Although different

scenarios were proposed to explain such effect on distinct systems, all ZEB materials reported so far have the reentrant spin glass-like (RSG) behavior as a common feature, which is characterized by an SG-like state concomitant with conventional magnetic phases [3,6–9]. Due to their intrinsic inhomogeneity, double-perovskite (DP) compounds usually present structural and magnetic disorder [10,11], being thus prospective candidates for exhibiting RSG behavior and the ZEB effect. Indeed, the majority of observed ZEB materials present perovskite structure [7,12–16].

The $La_{1.5}Sr_{0.5}CoMnO_6$ (LSCMO) compound stands out as having the largest ZEB effect reported so far [13]. In addition, it was observed that replacing Sr with Ca [$La_{1.5}Ca_{0.5}CoMnO_6$ (LCCMO)] also gives rise to an RSG material presenting the ZEB effect; however its $M(H)$ loop shift is one order of magnitude smaller than that of the Sr-based compound [14]. This difference can be understood, because structural, electronic, and magnetic properties are strongly intercorrelated in DP systems [10,11]; small differences in any of these properties could critically affect the ZEB effect.

Although the RSG behavior is a common feature of all ZEB materials, the microscopic mechanisms responsible for such effect are not fully understood. In this respect, the present work studies two DPs (LSCMO and LCCMO), which are representative examples of RSG and ZEB materials. Comprehensive magnetization measurements as a function of applied magnetic field and time [$M(H, t)$] were carried out, in order to shed light on the role played by the glassy magnetic phases on the ZEB effect. For comparison, we have also investigated the La_2CoMnO_6 (LCMO) DP, which is a non-RSG and non-ZEB material [17–19]. Our results clearly indicate that the coupling between the SG-like, FM, and AFM phases is paramount for the appearance of the ZEB effect. The different magnetic properties observed for the RSG DP compounds are discussed mainly in terms of the magnetic relaxation of the SG-like phase

*lbufaical@ufg.br

dynamics, which we describe by a proposed phenomenological model. This model predicts the horizontal shift observed in the $M(H)$ loops, with good agreement between experimental and calculated results, indicating that the time-evolution of the SG-like magnetization plays an important role in the ZEB effect.

II. EXPERIMENTAL DETAILS

Polycrystalline samples of LSCMO, LCCMO, and LCMO were synthesized by conventional solid state reaction, as described in the Supplemental Material (SM) [20]. X-ray powder diffraction patterns revealed the formation of single-phase DP structures for all compounds. The Rietveld refinement has indicated that LCMO and LCCMO grow in the monoclinic $P2_1/n$ space group [14], while LSCMO forms in the rhombohedral R-$3c$ space group, in agreement with previous reports [13].

Magnetic measurements were carried out using a Quantum Design PPMS-VSM magnetometer. All $M(H)$ loops were performed at $T = 5$ K up to a maximum magnetic field of $H_{max} = \pm 90$ kOe. Since both the SG-like behavior and the EB effect are extremely sensitive to the cooling process [24], we followed the same protocol for each measurement performed on all investigated samples. For each measurement, the system was slowly zero-field-cooled (ZFC) from the paramagnetic state down to $T = 5$ K, followed by a 10 minute wait time, to guarantee the thermal stabilization. From one measurement to another the sample was warmed up to the paramagnetic state and the coil was demagnetized in the oscillating mode, in order to prevent the presence of trapped current on the magnet and ensure a reliable ZFC process.

III. RESULTS AND ANALYSIS

A. Experimental results

The magnetization (M) of SG-like systems exhibits an unusual time dependence, which can lead to intriguing phenomena such as aging, rejuvenation, and memory effects [1–3]. Hence, it is expected that $M(H)$ loops measured with different H sweep rate (dH/dt) might lead to distinct M relaxation of the SG-like phase, which consequently affects the ZEB effect. We measured $M(H)$ loops for both LSCMO and LCCMO samples in ZFC mode, with $|dH/dt| = 150$ Oe/s; see Fig. 1(a) for the LSCMO compound. The measurement shows a clearly closed $M(H)$ loop, symmetric with respect to the M axis and shifted to the left along the H axis, as evidenced in the inset. These $M(H)$ loops are a superposition of three different magnetic phase contributions, namely, the hysteresis, due to the FM and SG-like phases, overlapped with a linear H-dependent contribution given by the AFM phase [3,13]. The shift along the H axis is a measure of the EB field, herein defined as $H_{EB} = |H^+ + H^-|/2$, where H^+ and H^- are the positive and negative coercive fields, respectively. For LSCMO we obtained $H_{EB}^{exp} = 3127$ Oe, while LCCMO showed $H_{EB}^{exp} = 165$ Oe (see SM [20]). The H values are herein approximated to integer numbers, and the experimental errors are neglected. Since M depends on H, which in turn depends on time (t), Fig. 1(a) can be displayed as a function of time [$M(t)$], see Fig. 1(b), which is suitable to our purpose of understanding how the dynamics of the SG-like phase act on the ZEB effect.
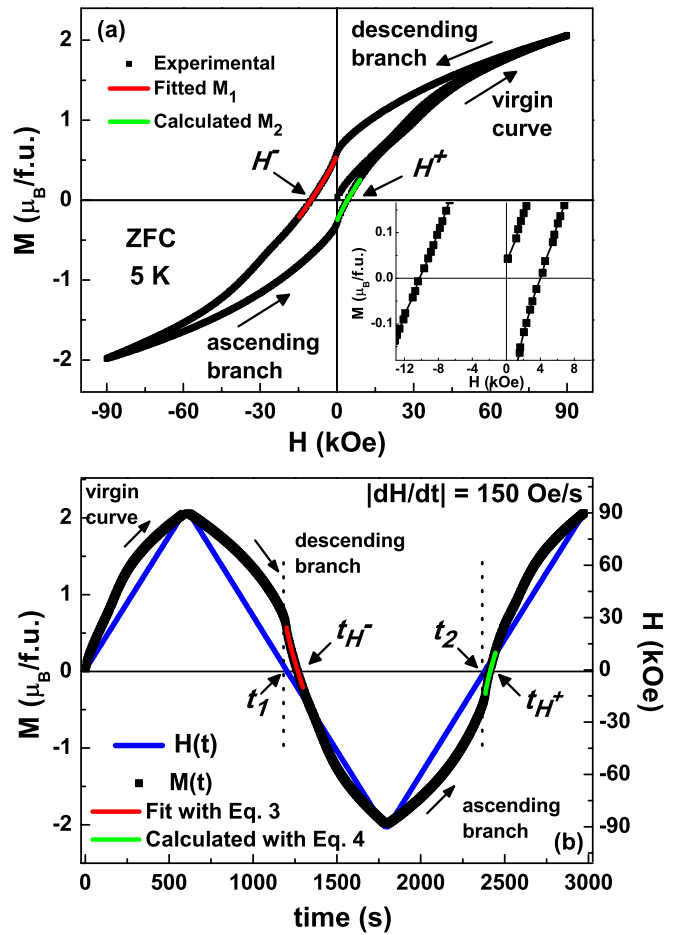

FIG. 1. (a) $M(H)$ loop of LSCMO at $T = 5$ K and $|dH/dt| = 150$ Oe/s. Red and green solid lines are the calculated M_1 [Eq. (4)] and M_2 [Eq. (5)] stretches, respectively. Inset shows zoom-in around $M = 0$, evidencing the shift along the H axis. (b) The same hysteresis loop for LSCMO, now displayed in $M(t)$ mode. The blue solid line is the magnetic field time dependence.

Evidence that the ZEB effect is critically affected by the SG-like phase is the fact that H_{EB} changes significantly depending on $|dH/dt|$. For LSCMO, an $M(H)$ loop with $|dH/dt| = 100$ Oe/s leads to $H_{EB}^{exp} = 3100$ Oe, lower than $H_{EB}^{exp} = 3127$ Oe obtained with $|dH/dt| = 150$ Oe/s. For $|dH/dt| = 50$ Oe/s, the shift decreases even further to $H_{EB}^{exp} = 2980$ Oe. Interestingly, for LCCMO the opposite trend was observed. $M(H)$ loops with $|dH/dt| = 50$, 100, and 150 Oe/s resulted in $H_{EB}^{exp} = 165$, 173, and 185 Oe, respectively. See Table I.

Glassy magnetic systems present a very long-lasting M relaxation. Therefore, to attest to the influence of the SG-like phase on the ZEB effect, we pause the $M(H)$ loop at a given magnetic field value for a time interval, leading to the relaxation of the magnetization, and subsequently completing the loop.

First we chose to pause $M(H)$ loops, with $|dH/dt| = 150$ Oe/s, at $H = 0$ on the descending branch, which is herein defined as an isothermal remnant M relaxation [IRM(t)] [lower inset of Fig. 2(a)] [25]. Moreover, we also pause at $H = 0$ on the ascending branch, as depicted in Fig. 2(a). The wait times were the same for both branches, for time intervals of $t_w = 600$,

TABLE I. Fitted [Eqs. (1), (3), and (4)] and calculated [Eq. (5)] parameters obtained from IRM(t) and $M(H)$ measurements for LSCMO and LCCMO. The goodness-of-fit parameters χ_1^2 and χ_3^2 represent the reduced χ^2 of the fittings with Eqs. (1) and (4), respectively.

| Sample	$\lvert dH/dt \rvert$ (Oe/s)	M_{sp} (μ_B/f.u.)	M_0 (μ_B/f.u.)	t_p (s)	n	χ_1^2	A (μ_B/f.u.)	B (μ_B/f.u.)	χ_3^2	r	t_1 (s)	t_2 (s)	$t_{H^-}^{exp}$ (s)	$t_{H^+}^{exp}$ (s)	$t_{H^+}^{calc}$ (s)	H_{EB}^{exp} (Oe)	H_{EB}^{calc} (Oe)
LSCMO	50	0.266	0.361	1.908×10^{11}	0.098	1.2×10^{-4}	0	0.008	5.4×10^{-4}	0.806	3524.1	7053.9		7113.7	7137.4	3072	2980
	100	0.262	0.362	1.924×10^{11}	0.096	2.4×10^{-4}	0	0.013	1.8×10^{-5}	0.814	1775.1	3554.5	1876.9	3594.5	3594.3	3090	3100
	150	0.258	0.358	3.634×10^{11}	0.094	3.6×10^{-4}	0	0.017	4.8×10^{-5}	0.837	1197.6	2385.2	1266.3	2412.5	2412.2	3105	3127
LCCMO	50	0.855	0.110	652.0	0.359	3.0×10^{-4}	0.0029	3.4×10^{-4}	3.8×10^{-6}	1.373	3517.2	7045.8	3691	7212.2	7209.5	185	253
	100	0.854	0.099	310.7	0.391	5.9×10^{-4}	−0.034	0.038	1.3×10^{-5}	1.034	1792.8	3572.4	1881.4	3657.7	3657.1	173	195
	150	0.854	0.099	236.6	0.398	8.8×10^{-4}	−0.027	0.034	1.4×10^{-5}	1.052	1195.8	2383	1254.7	2440	2439.9	165	173
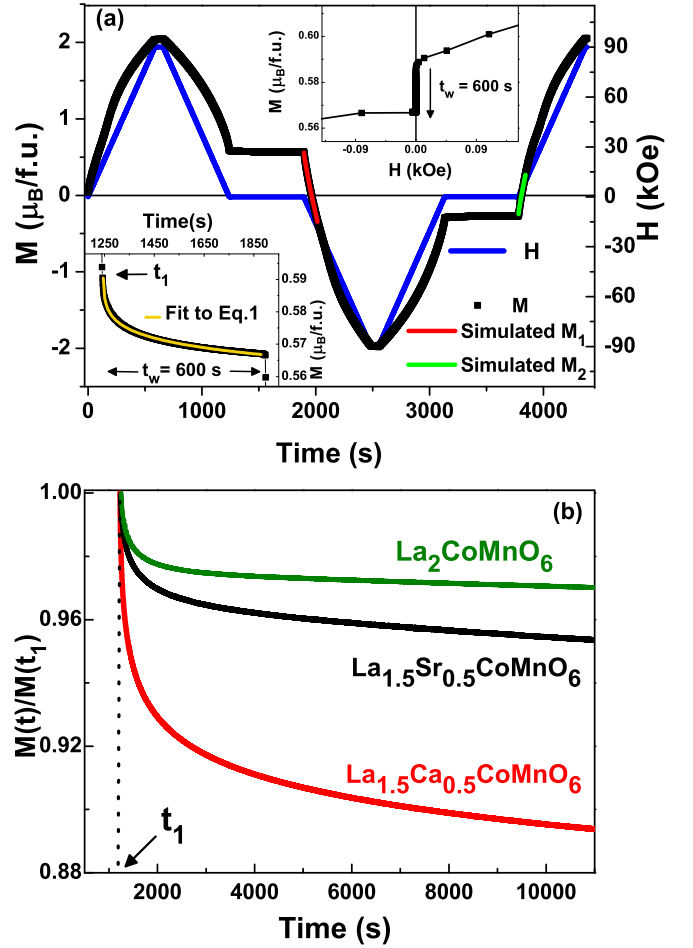
FIG. 2. (a) $M(t)$ curve of LSCMO ($T = 5$ K, $\lvert dH/dt \rvert = 150$ Oe/s), paused at $H = 0$ for a time interval $t_w = 600$ s, in the ascending and descending branches. Red and green lines are M_1 [Eq. (6)] and M_2 [Eq. (7)] stretches, respectively. The blue solid line is the magnetic field time dependence. The insets evidence the descending branch M decay at $H = 0$ in both $M(H)$ (upper inset) and $M(t)$ (lower inset) modes, and the yellow solid line shows the fitting of the M decay at $H = 0$ with [Eq. (1)]. (b) Normalized M decay for $t_w = 10^4$ s for LSCMO and LCCMO RSG samples, and for LCMO non-RSG and non-ZEB sample.

3600, and 10^4 s. In these cases, SG-like spins are expected to relax in a way to decrease the magnetization, thus reducing both $\lvert H^- \rvert$ and H^+. As will be discussed later, the effect of SG-like relaxation is stronger on the descending branch and consequently the decrease of $\lvert H^- \rvert$ is more pronounced. This results in a systematic reduction of H_{EB}^{exp} as t_w increases. The observed values for LSCMO H_{EB}^{exp} were 3082, 3060, and 3045 Oe for $t_w = 600$, 3600, and 10^4 s, respectively, as can be verified in Fig. 2(a) [displayed in $M(t)$ mode for $t_w = 600$ s]. The same trend was observed for LCCMO, i.e., the decrease of the ZEB effect as a function of t_w, from $H_{EB}^{exp} = 165$ Oe ($t_w = 0$) to 157 Oe ($t_w = 600$ s), 98 Oe ($t_w = 3600$), and 83 Oe ($t_w = 10^4$) (see SM [20]).

One might argue that the decrease of H_{EB}^{exp} could be explained by changes in other than the SG-like phase. Nevertheless, a remarkable feature of SG-like system is that, even for the longest t_w, the magnetization is expected to
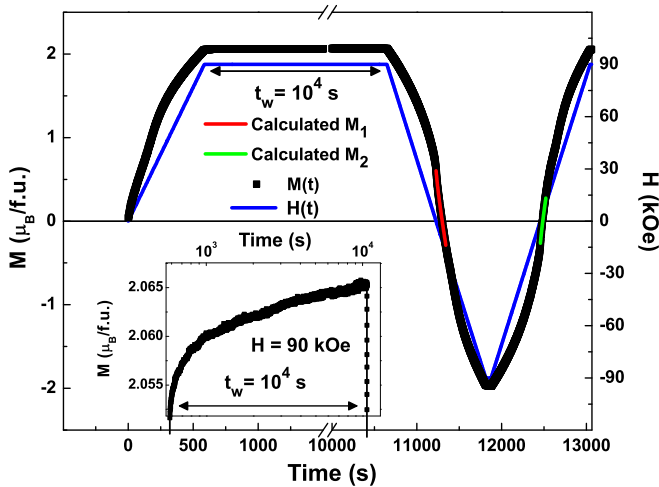
FIG. 3. $M(t)$ curve of LSCMO ($T = 5$ K, $|dH/dt| =$ 150 Oe/s), paused at $H_{max} = 90$ kOe for a time interval $t_w = 10^4$ s. Red and green solid lines are the calculated M_1 [Eq. (4)] and M_2 [Eq. (5)] stretches, respectively. The inset evidences the M relaxation at $H_{max} = 90$ kOe. The blue solid line is the magnetic field time dependence.

decay continuously [1–3]. Then, in order to distinguish the M-decay behavior from that of a conventional ferromagnetic system, we also investigated the t_w effect in the $M(H)$ loop of LCMO material. This FM insulator DP was extensively investigated due to its room-T magnetodielectric properties, and it presents no RSG behavior, or EB effect [17–19,26,27]. Figure 2(b) shows the normalized M decay [$M(t)/M(t_1)$] at the descending branch for $t_w = 10^4$ s curves for all samples. As can be noted, $M(t)/M(t_1)$ rapidly drops to a nearly constant value for the non-RSG sample, while it keeps continuously decreasing for the RSG samples, in a faster rate for the Ca-based material. H_{EB}^{exp} continuously decreases as t_w increases in LSCMO and LCCMO RSG samples, while for LCMO conventional magnetic material no loop shift was observed (see SM [20]). These results are strong evidence of the influence of the SG-like phase on the ZEB effect.

We now paused the $M(H)$ loop at the end of the virgin branch ($H_{max} = 90$ kOe), and subsequently completed the loop. Figure 3 displays the $M(t)$ curve obtained for $t_w = 10^4$ s on LSCMO, where the inset highlights the $M(t)$ relaxations at $H_{max} = 90$ kOe. The SG-like phase M relaxation certainly affects the loop (on both descending and ascending branches), but since the loop was paused only at $H = 90$ kOe, H^- is expected to vary more significantly than H^+, leading to the increase of H_{EB}. For LSCMO, $|dH/dt| = 150$ Oe/s, and $t_w =$ 600, 1800, 3600, and 10^4 s, H_{EB}^{exp} is enhanced to 3198, 3326, 3396, and 3527 Oe, respectively. The same overall behavior was observed for LCCMO, for which the measurements with $t_w = 0$, 600, 1800, 3600, and 10^4 s resulted in $H_{EB}^{exp} = 165$, 188, 227, 270, and 292 Oe, respectively [20].

In order to ensure that there are no extrinsic artifacts affecting the measurements, such as trapped current in the superconducting coils, we performed the same protocol described above, with $t_w = 10^4$ s, for a palladium standard, as well as the non-ZEB LCMO samples. The $M(H)$ curves obtained for these materials are symmetric in relation to the

horizontal and vertical axis, giving further evidence that the ZEB effect observed is related to the RSG behavior and not to trapped flux in the magnet; see SM [20].

All these results obtained for both samples can be readily understood in terms of our phenomenological model, which is based on the pinning and magnetic relaxation of the SG-like moments. According to it, changes in $|dH/dt|$ affect the relaxation of the SG-like spins and the balance between the SG-like, FM, and AFM phases present in the systems. As will be discussed below, these variations have a direct impact on H^+ and H^-, and consequently on H_{EB}.

B. The ZEB model

An usual EB effect is explained in terms of the coupling between two different magnetic phases, one of pinned moments and the other with reversing spins, which are being driven by the applied magnetic field. Similarly, our model for ZEB systems is based on the coupling between the reversing spins of the FM phase with the pinned spins of the SG-like phase. In an $M(H)$ loop of a ZEB material, for instance, in the descending branch for $H < 0$, due to the relatively slow relaxation, not all spins of the SG-like phase will be flipped toward the negative field direction. Some of the moments will still point toward the positive H_{max} field previously applied.

In Fig. 1(b), t_1 and t_2 represent the times when $H = 0$, while t_{H^-} and t_{H^+} correspond to the instants when $M = 0$ (in the descending and ascending branches, respectively). The magnetization at the t interval $t_1 \leqslant t \leqslant t_{H^-}$ is defined as M_1 stretch, and the $t_2 \leqslant t \leqslant t_{H^+}$ interval as M_2 stretch. A key point of our phenomenological model is how the dynamics of the SG-like moments are affected by the magnetic history of the $M(H)$ loop. The amount M_{SG} pinned on the opposite H direction will change asymmetrically in M_1 and M_2 stretches, due to their magnetic history; i.e., while the M_1 stretch history is associated with the virgin curve and half of the descending branch, M_2 is correlated with the virgin branch, the whole descending, and half of the ascending branches.

To compute how the SG-like phase may affect the hysteresis loop, we estimated the stretches of the $M(H)$ curves between $H = 0$ and $M = 0$ (i.e., the regions encompassing M_1 and M_2 in the descending and ascending branches, respectively). To calculate both stretches, the following steps were followed: (i) the magnetization's time evolution of the SG-like phase was taken into account; (ii) the time evolution of the AFM and FM phases due to the applied magnetic field was also considered; (iii) from the parameters obtained in steps (i) and (ii), the magnetization of each stretch was calculated. For the ascending branch stretch, it was assumed, as an approximation, that nearly half of the SG-like moments had flipped toward the negative H direction, while the other half is relaxing but still pointed toward the opposite direction. From the resulting calculated curves, H^+ and H^- could be computed, allowing the estimation of H_{EB}.

The first step considers the dynamics of the SG-like phase during the $M(H)$ loop measurement. The time evolution of SG systems has been extensively debated in the last decades. Many models have been proposed to describe curves like the IRM(t) [see Ref. [25] and the lower inset of Fig. 2(a)]. The stretched exponential model is generally admitted to be the most relevant

to account for these curves in conventional SG materials [1,3]. Given that we are not dealing here with canonical SG, but with RSG materials, which exhibit a non-negligible contribution to the magnetization from the FM phase, a term must be added to the stretched exponential equation in order to account for this contribution, yielding

$$M_{SG}(t) = M_{sp} + M_0 e^{-[(t-t_1)/t_p]^n}, \qquad (1)$$

where M_{sp} corresponds to the spontaneous magnetization of the FM phase, M_0 is the initial magnetization of the SG-like phase at the instant t_1, and finally, t_p and n ($0 < n < 1$) are the time and the time-stretch exponential constants, respectively. The parameters obtained from the fit of the experimental IRM(t) curve with Eq. (1) are displayed in Table I.

As stated above, to compute the M_1 and M_2 stretches, the effect of $|dH/dt|$ on the FM and AFM phases must be taken into account. Several functional forms have been proposed to fit the hysteresis curves of magnetic materials and, in general, each compound is better described by a particular model; i.e., there is not a universal equation that models $M(H)$ loops [28]. Since our purpose is not to understand microscopically how the magnetic field affects the AFM and FM phases, but only to fit the contribution from these phases to M_1 and M_2, our choice was for the simplest model. Thus, the following equation is suitable for our purpose:

$$M_m(H) = A'H + B'H^r. \qquad (2)$$

In this equation, A' is related to the linear H dependence of the AFM phase, and B' and r account for the nonlinear contribution of the FM phase to magnetization.

Alternatively, since the field sweep rate (dH/dt) is constant, we can rewrite the above expression as a function of time,

$$M_m(t) = At + Bt^r, \qquad (3)$$

where now, A and B are proportional to A' and B', and r is the same as Eq. (2).

Our approximate model considers that in the time-interval $t_1 \leqslant t \leqslant t_{H^-}$ the system is relaxing due to the positive H_{max} applied before, but it is already under the effect of a linearly varying negative H. Therefore, the equation describing the M_1 stretch is

$$M_1(t) = \{M_{sp} + M_0 e^{-[(t-t_1)/t_p]^n}\}$$
$$- \{A(t - t_1) + B(t - t_1)^r\}. \qquad (4)$$

The first pair of braces corresponds to the SG-like phase's relaxation from the previously applied positive H_{max}, with the same parameters of Eq. (1). The second pair of braces accounts for the influence of the immediately applied negative H. In order to evaluate the parameters of the second pair of braces, we kept fixed those obtained from the fitting of Eq. (1).

Figure 4(a) shows the fitting of M_1 with Eq. (4) for the $M(H)$ curve of LSCMO with $|dH/dt| = 150$ Oe/s, where one can see a very good agreement between the fitted and experimental results. The parameters obtained from the fitting are displayed on Table I. As can be noted from Table I, A is negligible for any $|dH/dt|$ of the LSCMO sample, indicating
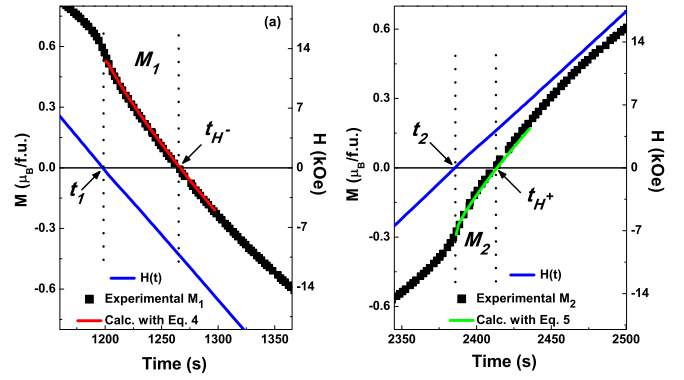

FIG. 4. Magnified view of the experimental and calculated M_1 (a) and M_2 (b) stretches of the $M(H)$ curve obtained for LSCMO at $T = 5$ K and $|dH/dt| = 150$ Oe/s. The blue solid line is the magnetic field time dependence.

that around H^- the FM contribution is much larger than the AFM one.

Now, with the parameters obtained for the FM, AFM, and SG-like phases, the M_2 stretch can be calculated. Here our approximate assumption is that when the negative field is applied, not all SG-like moments have been flipped toward negative direction, but half are still relaxing from the positive field previously applied. Hence, the equation for M_2 becomes

$$M_2(t) = -\left\{M_{sp} + \frac{M_0}{2}e^{-[(t-t_2)/t_p]^n}\right\} + \left\{\frac{M_0}{2}e^{-[(t-t_1)/t_p]^n}\right\}$$
$$+ \{A(t - t_2) + B(t - t_2)^r\}, \qquad (5)$$

where the first pair of braces represents the decay of the SG-like spins that are relaxing from the negative field applied before, the second pair corresponds to the relaxation from the positive field previously applied, and the third pair represents the variation in the AFM/FM phases due to the just applied positive field. The decay of the SG-like moments pointing toward the positive direction starts at t_1, while the decay of those pointing toward the negative direction starts at t_2. Also, the FM phase spontaneous magnetization M_{sp} is assumed to have been flipped toward the negative direction due to the $H = -90$ kOe previously applied. Using the parameters obtained from Eqs. (1) and (3), the M_2 stretch can be calculated. As can be seen in Fig. 4(b), the curve obtained from the model is very similar to the experimental result. From the calculation of M_2 with Eq. (5) one gets $t_{H^+}^{calc} = 2412.5$ s, yielding $H_{calc}^+ = 150 \times (t_{H^+}^{calc} - t_2) = 4095$ Oe. Combining it with $H^- = -10\,305$ Oe obtained from the M_1 stretch, one gets $H_{EB}^{calc} = 3105$ Oe, which is close to the experimentally observed value $H_{EB}^{exp} = 3127$ Oe. It must be stressed that the theoretical curve of Fig. 4(b) is not a fitting to the experimental M_2, but a calculated curve for which the parameters obtained from Eqs. (1) and (4) were kept fixed.

Once again, it must be emphasized that the above described model is an approximation that does not intend to perfectly describe the microscopic mechanism responsible for the complex magnetic behavior of the investigated systems, but only to shed some light on the ZEB effect and evidence the

role played by the SG-like phase. There are several possible sources of discrepancies of our model to the real system, many of them being related to dynamics of the SG-like phase itself, but also to instrumental sources of imprecision (see SM [20]). Nevertheless, despite the above mentioned sources of imprecision, the proximity between the calculated and experimental results is remarkable.

Significant evidence of the validity of our model is that, according to it, H_{EB} is expected to vary for different $|dH/dt|$. One can observe in Table I that both parameters of Eq. (1), the n exponent and t_p, change with $|dH/dt|$. These parameters govern the relaxation rate of the SG-like phase. For smaller/larger n, slower/faster will relax the magnetization [3], which increases/decreases both $|H^-|$ and H^+ in our model. However, since in Eq. (5) the two terms containing n have opposites signs, the increase/decrease is always larger on $|H^-|$ than on H^+. Therefore, decreasing/increasing n will lead to an enhancement/diminishment of H_{EB}. Although the H_{EB} of LSCMO and LCCMO have opposite trends in respect to dH/dt, our model captures the interplay between SG-like magnetization relaxation and exchange bias.

We can understand the observed values of H_{EB} as a counterbalance between $|dH/dt|$, the relaxation of the SG-like phase, and the magnetic history of the $M(H)$ loop. We can think that the magnetic history of the magnetization loop is imprinted in the M_{SG}. So, a slow/fast SG-like relaxation corresponds to keeping an old/fresh memory of the magnetization loop history. The magnetic history of the M_1 stretch, and therefore of H^-, is quite different from those of M_2 and H^+. Depending on how old/fresh the memory is, larger/smaller will be the loop asymmetry, implying larger/smaller H_{EB} values. Since both t_p and n indicate that the magnetization relaxation is slower for LSCMO than for LCCMO, this corresponds to an older memory; the H_{EB} for the first should be larger than for the latter.

Our ZEB phenomenological model can also describe the change in H_{EB} observed for the measurements where $M(H)$ loops were paused for a given interval t_w at $H_{max} = 90$ kOe. In Fig. 5(a) are shown the IRM(t) curves obtained for LSCMO for different t_w. Clearly, the magnetization increases as t_w increases, leading to the increment of M_0 and M_{sp} (see SM [20]). It can also be noted that the curve's slope does not change significantly for different t_w, since it affects mainly the amount of SG-like phase, while the parameters of Eq. (3) remain nearly the same. In this case, the M_1 and M_2 stretches are also calculated using Eqs. (4) and (5), as done for $M(H)$ loops for $t_w = 0$, but keeping A, B, and r parameters fixed with the values obtained for $t_w = 0$. Figures 5(b) and 5(c) show the evolution of experimental and calculated H_{EB} and $|H^-|$ with increasing t_w. It is worth noting that the M_1 stretch is no longer a fitting, but a calculation, which checks the model strength and allows a direct observation of the influence of the SG-like phase on the EB effect. Although there are quantitative differences between the experimental and calculated values, our model captures the H_{EB} trend observed. For LCCMO, the same overall behavior was found [20].

For experiments pausing at $H = 0$ with different t_w, all parameters were kept fixed at the values obtained from the $t_w = 0$ curve. The M_1 and M_2 stretches were calculated from
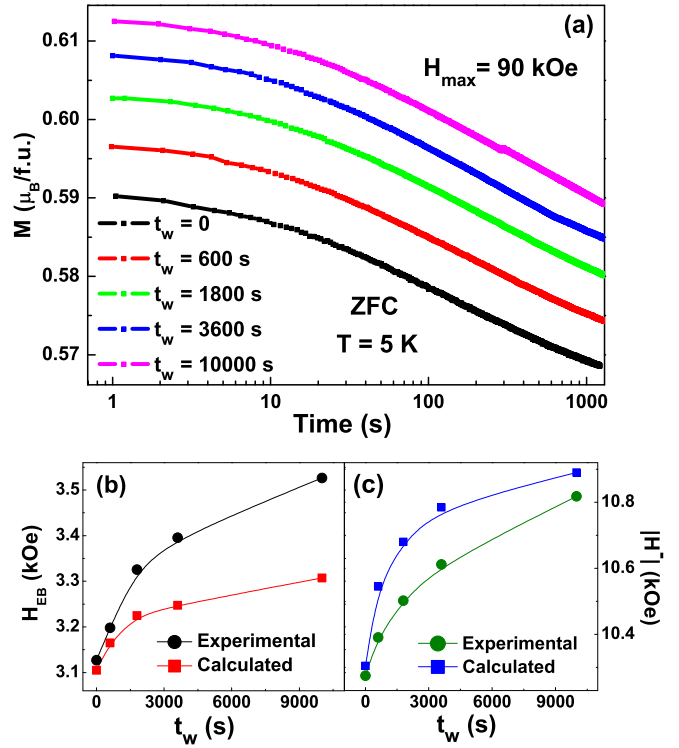

FIG. 5. (a) IRM(t) curves for LSCMO at $T = 5$ K and $|dH/dt| = 150$ Oe/s, for different t_w at $H_{max} = 90$ kOe. (b) and (c) show the evolution of H_{EB} and $|H^-|$ as a function of t_w, respectively. The solid lines are guides for the eye.

modified Eqs. (4) and (5), in which we take into account the effect of t_w on the SG-like phase, yielding

$$M_1(t) = \{M_{sp} + M_0 e^{-[(t-t_1)/t_p]^n}\}$$
$$- \{A[t - (t_1 + t_w)] + B[t - (t_1 + t_w)]^r\}, \quad (6)$$

$$M_2(t) = -\left\{M_{sp} + \frac{M_0}{2} e^{-[(t-t_2)/t_p]^n}\right\} + \left\{\frac{M_0}{2} e^{-[(t-t_1)/t_p]^n}\right\}$$
$$+ \{A[t - (t_2 + t_w)] + B[t - (t_2 + t_w)]^r\}. \quad (7)$$

The M_1 and M_2 curves calculated with Eqs. (6) and (7) agree very well with the experimental results, as can be seen in Fig. 2(a).

In this case, we observed a decrease of H_{EB} as a function of t_w, related to the reduction of both $|H^-|$ and H^+; see Figs. 6(a) and 6(b). This can be understood as a partial refresh of the memory imprinted on the M_{SG} by the magnetic history, when the loop is paused at $H = 0$. In both descending and ascending branches, during the time interval t_w the SG-like magnetization relaxes exponentially toward zero. Once the exchange bias is due to the coupling between the FM and SG-like phases, and considering that the latter decreases, it is expected that H_{EB} will decrease as well. In the limiting situation, pausing at $H = 0$ for an infinite time, or alternatively, for a very fast M_{SG} relaxation, the memory will be completely erased, and H_{EB} will be zero.
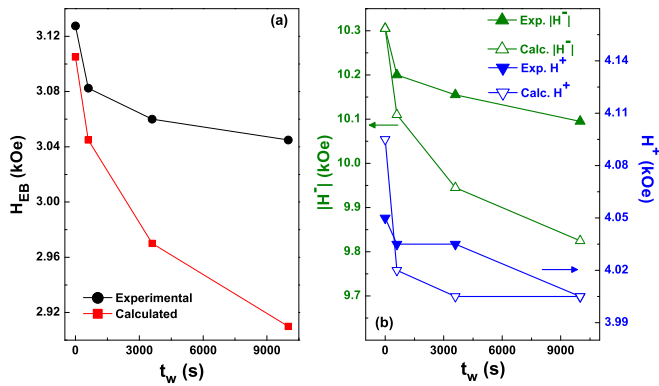
FIG. 6. Experimental and calculated (a) H_{EB} and (b) H^+ and $|H^-|$ as a function of t_w obtained from the $M(H)$ loops of LSCMO in which the experiment was paused at $H = 0$. The solid lines are guides for the eye.

IV. SUMMARY

In summary, we have investigated in detail the dynamics of magnetization for two RSG compounds that are representative ZEB materials: $La_{1.5}Sr_{0.5}CoMnO_6$ and $La_{1.5}Ca_{0.5}CoMnO_6$. Different experiments were carried out to elucidate how the SG-like phase influences the ZEB effect. For comparison, the magnetic properties of the non-RSG and non-ZEB La_2CoMnO_6 compound were also investigated. We found strong evidence that the unusual magnetic relaxation of the glassy moments is strongly correlated with the loop shifts. We also propose a simple phenomenological model, based on the fractionated flipping of the SG-like spins and on their unusual dynamics, to describe the ZEB effect. The calculated results agree with the experimental values. Based on the model, the large difference between the ZEB effect observed for $La_{1.5}Sr_{0.5}CoMnO_6$ and $La_{1.5}Ca_{0.5}CoMnO_6$ could be explained in terms of magnetization relaxation of the SG-like phase. Although it must be checked for other ZEB materials, the model indicates that the dynamics of the SG-like phases present on these RSG systems is key to the emergence of ZEB effect.

[1] K. H. Fischer and J. A. Hertz, *Spin Glasses* (Cambridge University Press, Cambridge, 1991).

[2] D. L. Stein and C. M. Newman, *Spin Glasses and Complexity* (Princeton University Press, Princeton, 2013).

[3] J. A. Mydosh, *Spin Glasses: An Experimental Introduction* (Taylor & Francis, London, 1993).

[4] J. Nogués and I. K. Schuller, J. Magn. Magn. Mater. **192**, 203 (1999).

[5] E. Dagotto, Science **318**, 1076 (2007).

[6] B. M. Wang, Y. Liu, P. Ren, B. Xia, K. B. Ruan, J. B. Yi, J. Ding, X. G. Li, and L. Wang, Phys. Rev. Lett. **106**, 077203 (2011).

[7] T. Maity, S. Goswami, D. Bhattacharya, and S. Roy, Phys. Rev. Lett. **110**, 107201 (2013).

[8] A. K. Nayak, M. Nicklas, S. Chadov, C. Shekhar, Y. Skourski, J. Winterlik, and C. Felser, Phys. Rev. Lett. **110**, 127204 (2013).

[9] F. Tian, K. Cao, Y. Zhang, Y. Zeng, R. Zhang, T. Chang, C. Zhou, M. Xu, X. Song, and S. Yang, Sci. Rep. **6**, 30801 (2016).

[10] S. Vasala and M. Karpinnen, Prog. Solid State Chem. **43**, 1 (2015).

[11] D. Serrate, J. M. De Teresa, and M. R. Ibarra, J. Phys.: Condens. Matter **19**, 023201 (2007).

[12] L. T. Coutrim, E. M. Bittar, F. Stavale, F. Garcia, E. Baggio-Saitovitch, M. Abbate, R. J. O. Mossanek, H. P. Martins, D. Tobia, P. G. Pagliuso, and L. Bufaiçal, Phys. Rev. B **93**, 174406 (2016).

[13] J. Krishna Murthy and A. Venimadhav, Appl. Phys. Lett. **103**, 252410 (2013).

[14] L. Bufaiçal, R. Finkler, L. T. Coutrim, P. G. Pagliuso, C. Grossi, F. Stavale, E. Baggio-Saitovitch, and E. M. Bittar, J. Magn. Magn. Mater. **433**, 271 (2017).

[15] S. Huang, L. R. Shi, Z. M. Tian, H. G. Sun, and S. L. Yuan, J. Magn. Magn. Mater. **394**, 77 (2015).

[16] L. Xie and H. G. Zhang, Curr. Appl. Phys. **18**, 261 (2018).

[17] M. P. Singh, K. D. Truong, and P. Fournier, Appl. Phys. Lett. **91**, 042504 (2007).

[18] T. Burnus, Z. Hu, H. H. Hsieh, V. L. J. Joly, P. A. Joy, M. W. Haverkort, Hua Wu, A. Tanaka, H.-J. Lin, C. T. Chen, and L. H. Tjeng, Phys. Rev. B **77**, 125124 (2008).

[19] L. López-Mir, R. Galceran, J. Herrero-Martín, B. Bozzo, J. Cisneros-Fernández, E. V. Pannunzio Miner, A. Pomar, L. Balcells, B. Martínez, and C. Frontera, Phys. Rev. B **95**, 224434 (2017).

[20] See Supplemental Material at http://link.aps.org/supplemental/10.1103/PhysRevB.98.064426 for details of the crystal growth, magnetization measurement, and calculations with the proposed equations. It includes Refs. [21,22,23].

[21] A. C. Larson and R. B. Von Dreele, General Structure Analysis System (GSAS), Los Alamos National Laboratory Report LAUR 86–748 (2004).

[22] J. Krishna Murthy, K. D. Chandrasekhar, H. C. Wu, H. D. Yang, J. Y. Lin, and A. Venimadhav, J. Phys.: Condens. Matter **28**, 086003 (2016).

[23] M. H. Frey and D. A. Payne, Phys. Rev. B **54**, 3158 (1996).

[24] N. J. Gökemeijer and C. L. Chien, J. Appl. Phys. **85**, 5516 (1999).

[25] Conventionally, to measure the remnant magnetization of a SG material as a function of t, the system is cooled in the presence of a small H, which is suppressed at $T < T_{sg}$ and then M is computed as a function of t. Since our purpose here is to model ZFC $M(H)$ loops, the following protocol was adopted to measure IRM(t) curves: First the system was ZFC down to 5 K. Then H was increased up to 90 kOe and subsequently

decreased down to zero. After this protocol, M was measured as a function of t. Note that this protocol, carried out prior to each IRM(t) measurement, corresponds to the virgin curve and the descending branch of an $M(H)$ loop.

[26] K. Manna, R. S. Joshi, S. Elizabeth, and P. S. Kumar, Appl. Phys. Lett. **104**, 202905 (2015).

[27] J. Krishna Murthy, K. D. Chandrasekhar, S. Murugavel, and A. Venimadhav, J. Mater. Chem. C **3**, 836 (2015).

[28] F. C. Trutt, E. A. Erdélyi, and R. E. Hopkins, IEEE Trans. on Powder Apparatus and Systems **PAS-87**, 665 (1968).